Quantum Electronics **47** (6) 580–588 (2017)

OPTICAL IMAGES

https://doi.org/10.1070/QEL16338

Measurement of an image jitter of an extended incoherent radiation source

V.P. Lukin, V.V. Nosov

Abstract. **A scheme of an image jitter measuring device, which uses an extended incoherent source as a radiation source, is presented. The efficiency of the measuring device is analysed analytically and numerically in order to justify the operation of the adaptive optical system that does not require special creation or formation of a reference source. The features of the formed image of incoherent radiation are considered, in particular from the point of view of its possible application for measuring the phase fluctuations of optical waves propagating in a turbulent atmosphere (the adaptive system monitors the image of a self-luminous object illuminated by extraneous sources). The possibility of utilising a Shack–Hartmann wavefront sensor in adaptive systems using the image of an arbitrary object (or its fragment) as a reference source is shown.**

Keywords: *correction, reference source, image, phase, coherence.*

1. Introduction

The problem of optical radiation transfer through a medium (atmosphere) arises in a number of practical applications, for example, in laser energy delivery. Inhomogeneities of a medium, including atmospheric turbulence, become a serious obstacle limiting the ultimately achievable characteristics and capabilities of astronomical telescopes and other optoelectronic systems (OES's) [1, 2], which construct an image. It is known that the use of adaptive optics (AO) systems allows these limitations to be substantially reduced [3–5]. However, in the practical application of algorithms and AO systems, one needs current information about the fluctuations in the characteristics of an optical wave. This information can be obtained, in particular, by using additional (reference) sources, which make it possible to measure distortions in a radiation propagation channel [6–8].

2. Reference source as an element of an AO system

Let us explain what a reference source is. On the one hand, in the theory of AO systems [6], this element is traditionally considered to be a model that allows limiting correction capabilitie to be estimated with the help of the AO system, and, on the other hand, it provides a real scenario for the operation of OES's using AO. Thus, a reference source provides the simulation of the AO system operation *in corpore*.

History of the development of adaptive optics itself is inextricably associated with the development of views on the use of reference sources in various OES's [9, 10]. This was especially evident in astronomical applications of AO systems when using so-called laser reference stars. It should be noted that the recent revision (see [11]) of the history of the development of views on the use of reference sources in astronomy – laser reference stars (reference sources formed with the help of laser radiation) – makes it impossible to determine the real contribution of the works of this or that author.

All work on the formation of reference stars with the help of laser radiation was initially classified in the US, and the first data were openly published only in the early 1993. The first publication should be considered a thematic issue of the Lincoln Laboratory Journal [12]. There had been no other open publications in the United States by this time, and one can be sure of this, for example, if one becomes acquainted with the programme and the texts of the reports at the famous Scintillation conference (Seattle, the USA, 3–7 August, 1992) [13]. At the same time, there were numerous open publications of Soviet researchers, who in particular studied the features of phase and intensity fluctuations of optical waves during a double passage through turbulence. A detailed scientific analysis of this problem and the first papers, which, in fact, led to the creation of the technique of laser reference stars, was given in monograph [10] (see Chapter 5). The first open western publication on the use of laser reference stars should be considered the work of Foy and Laberyrie in 1985 [14].

Already the first papers [7, 9, 10] on the use of specially created reference sources pointed to the possibility of using reflected waves. In this case, for example, such reference radiation can be the radiation reflected from the object itself, on which it is necessary to focus coherent laser radiation. A situation is possible when reference radiation produced by the 'illumination' of an object by a radiation beam from an additional source is used to provide the operation of a wavefront sensor of an AO system [15–21]. In this case, 'illumination' can be either coherent or incoherent. Methods for determining the phase with respect to both coherent and incoherent reference radiation have already been described in the scientific literature [7, 22, 23].

3. Calculation of the image intensity for an incoherent radiation source

In the present work, we calculate the distribution of the average intensity in the image plane of an incoherent object that is formed by the OES. The space between the incoherent radia-

V.P. Lukin, V.V. Nosov V.E. Zuev Institute of Atmospheric Optics, Siberian Branch, Russian Academy of Sciences, pl. Akad. Zueva 1, 634021 Tomsk, Russia; e-mail: lukin@iao.ru, nosov@iao.ru

Received 10 March 2017; revision received 12 April 2017
Kvantovaya Elektronika **47** (6) 580–588 (2017)
Translated by I.A. Ulitkin

tion source and the receiving aperture of the optical system is filled with a turbulent atmosphere that distorts the image being formed.

To eliminate turbulent distortions, use is made of an AO system which relies on a signal from a reference source. In our case, we suggest using an image of the most extended object as a reference source. With the help of the results of [18, 21], we write down the instantaneous image intensity distribution for an extended source of incoherent radiation generated through a turbulent medium in the approximation of the generalised Huygens–Kirchhoff method [2]:

$$\gamma(X_{\text{im}},\boldsymbol{\rho}) = \frac{1}{X^2 X_{\text{im}}^2}\iint \mathrm{d}^2 r_1 I_{\text{ob}}(X,\boldsymbol{r}_1)\iint \mathrm{d}^4\rho_{1,2}\exp(-\mathrm{i}k\rho_1^2/2f$$

$$+\mathrm{i}k\rho_2^2/2f)\,W(\boldsymbol{\rho}_1)\,W^*(\boldsymbol{\rho}_2)\exp\{\mathrm{i}k|\boldsymbol{\rho}-\boldsymbol{\rho}_1|^2/2X_{\text{im}}$$

$$-\mathrm{i}k|\boldsymbol{\rho}-\boldsymbol{\rho}_2|^2/2X_{\text{im}}+\mathrm{i}k|\boldsymbol{r}_1-\boldsymbol{\rho}_1|^2/2X-\mathrm{i}k|\boldsymbol{r}_1-\boldsymbol{\rho}_2|^2/2X\}$$

$$\times\exp\{\mathrm{i}[S(X,\boldsymbol{r}_1;0,\boldsymbol{\rho}_1)-S(X,\boldsymbol{r}_1;0,\boldsymbol{\rho}_2)]\}. \qquad (1)$$

Here, X is the length of the atmospheric path between an object and an OES; f is the focal length of the OES receiving device generating an image of an extended source object; X_{im} is the distance from the OES receiving aperture to the image plane; $I_{\text{ob}}(X,\boldsymbol{r})$ is the brightness distribution of the source object; $W(\boldsymbol{\rho})$ is the function of the pupil of the receiving lens of the system; $S(X,\boldsymbol{r}_1;0,\boldsymbol{\rho}_1)$ are the phase fluctuations due to the action of turbulence; and k is the wave number.

We shall analyse expression (1) in the so-called conjugate plane, i.e., in the plane for which the 'thin' lens approximation is valid:

$$1/f = 1/X_{\text{im}} + 1/X. \qquad (2)$$

Then, from (1) we obtain

$$\gamma(X_{\text{im}},\boldsymbol{\rho}) = \frac{1}{X^2 X_{\text{im}}^2}\iint \mathrm{d}^2 r_1 I_{\text{ob}}(X,\boldsymbol{r}_1)\iint \mathrm{d}^4\rho_{1,2}\,W(\boldsymbol{\rho}_1)\,W^*(\boldsymbol{\rho}_2)$$

$$\times\exp[-\mathrm{i}k\boldsymbol{r}_1(\boldsymbol{\rho}_1-\boldsymbol{\rho}_2)/X]\exp\{[-\mathrm{i}k\boldsymbol{\rho}(\boldsymbol{\rho}_1-\boldsymbol{\rho}_2)/X_{\text{im}}]$$

$$+\mathrm{i}[S(X,\boldsymbol{r}_1;0,\boldsymbol{\rho}_1)-S(X,\boldsymbol{r}_1;0,\boldsymbol{\rho}_2)]\}. \qquad (3)$$

To obtain expression (3) in [18, 21], the delta-correlation approximation for the coherence function of initial radiation was used. Next, we consider some features of the image (3) formed by incoherent radiation, in particular the possibility of using it to measure the phase fluctuations of optical waves propagating in a turbulent atmosphere.

4. Formulation of the Ehrenfest theorem for atmospheric-optical systems

In known papers [24, 25] it was shown that the problems of refraction of optical radiation in atmospheric-optical systems are virtually reduced to the calculation of various functionals of the quantity $\nabla_\rho\,\gamma(x,\boldsymbol{R},\boldsymbol{\rho})\big|_{\rho=0}$, where

$$\gamma(x,\boldsymbol{R},\boldsymbol{\rho}) = U(x,\boldsymbol{R}+\boldsymbol{\rho}/2)\,U^*(x,\boldsymbol{R}-\boldsymbol{\rho}/2); \qquad (4)$$

$\gamma(x,\boldsymbol{R},0) = I(x,\boldsymbol{R})$; $U(x,\boldsymbol{\rho})$ is the amplitude of the optical field, the intensity of which is given by expression (3).

Such a frequently measured characteristic, as the displacement vector of the energy centre of gravity of the optical radiation formed in the focal plane of the receiving device, can be represented in the form [25]:

$$\rho_{\text{t}} = -\frac{\mathrm{i}\lambda F_{\text{t}}}{2\pi c_{\text{t}}}\int \mathrm{d}^2 R\,T(\boldsymbol{R})\nabla_\rho\gamma(x,\boldsymbol{R},\boldsymbol{\rho})\big|_{\rho=0}, \qquad (5)$$

where $c_{\text{t}} = \int \mathrm{d}^2 R\,T(\boldsymbol{R})\gamma(x,\boldsymbol{R},0)$; $T(\boldsymbol{R})$ is the transmittance with respect to the intensity of the receiving device optics constructing an image (telescope); and F_{t} is the focal distance of the receiving device (telescope).

As is known from [2, 25], expression

$$\nabla_\rho\,\gamma(x,\boldsymbol{R},\boldsymbol{\rho})\big|_{\rho=0} = \mathrm{i}I(x,\boldsymbol{R})\nabla_R S(x,\boldsymbol{R}) \qquad (6)$$

relates the optical wave field $U(x,\boldsymbol{\rho})$ with its phase S and intensity I. This expression can easily be proved by differentiating the function $\gamma(x,\boldsymbol{R},\boldsymbol{\rho})$. It should be noted that, strictly speaking, the operation of differentiating the function $\gamma(x,\boldsymbol{R},\boldsymbol{\rho})$ can be performed only when the phase of the wave is a smooth analytic function. Then, in expression (5) for the vector $\boldsymbol{\rho}_{\text{t}}$, after differentiation under the integral, we can pass to the limit $\boldsymbol{\rho}\to 0$. Thus, this phase S is called analytic.

5. Singular phase of an optical wave and its regularisation. Basic relationships

In some regimes of wave propagation, its phase is strongly 'destroyed' and becomes a singular [25] function rather than an analytic one. These cases are usually characterised by a small radius ρ_{coh} of the spatial coherence of the field. If ρ_{coh} is much smaller than the effective radius of the beam itself, the width of the second-order coherence function $\Gamma_2(x,\boldsymbol{R},\boldsymbol{\rho}) = \langle\gamma(x,\boldsymbol{R},\boldsymbol{\rho})\rangle$ coincides with ρ_{coh} with respect to the difference coordinate $\boldsymbol{\rho}$, because $\Gamma_2(x,\boldsymbol{R},\boldsymbol{\rho})\approx\exp(-\rho^2/\rho_{\text{coh}}^2)$. Therefore, for $\rho_{\text{coh}}\to 0$, we can assume that $\Gamma_2(x,\boldsymbol{R},\boldsymbol{\rho})\approx\exp(-\rho^2/\rho_{\text{coh}}^2)\to\delta(\bar{\rho})$ [here $\delta(\bar{\rho})$ is the delta function]. We can show below that since the average value of $\gamma(x,\boldsymbol{R},\boldsymbol{\rho})$ coincides with the coherence function, then approximately $\gamma(x,\boldsymbol{R},\boldsymbol{\rho})\approx\delta(\boldsymbol{\rho})$. Consequently, for small radii of the field coherence (which is true for the case of the formation of radiation from an incoherent object), in computing $\nabla_\rho\,\gamma(x,\boldsymbol{R},\boldsymbol{\rho})\big|_{\rho=0}$ there arises an uncertainty of the singular type, namely:

$$\nabla_\rho\gamma(x,\boldsymbol{R},\boldsymbol{\rho})\big|_{\rho=0} = \nabla_\rho\,\delta(\boldsymbol{\rho})\big|_{\rho=0} = \nabla_\rho\delta^2(\boldsymbol{\rho}).$$

In situations when the last relationship is fulfilled, the phase of a light wave can be called singular. Hence, the singularity should be eliminated, or regularised.

Regularisation is necessary when describing an incoherent source and a focused beam, and also in the region of strong turbulent beam broadening. The simplest method of regularisation in the case of phase singularities is to change the order of the transition to the limits. To this end, the initial field, which is already described by the singular function $\gamma(x,\boldsymbol{R},\boldsymbol{\rho})$, must be represented as a superposition of elementary beams with an analytic phase [25]. The limit transition in this superposition (sum) with respect to some selected parameter must ensure that the superposition of these elementary beams is

close to the original singular beam. For each such elementary beam, the quantity $\nabla_\rho \gamma(x,\boldsymbol{R},\boldsymbol{\rho})\big|_{\rho=0}$ is no longer singular, and the order of the transition to the limits can be changed:

$$\nabla_\rho \gamma(x,\boldsymbol{R},\boldsymbol{\rho})\big|_{\rho=0} = \lim_{\rho\to 0}\nabla_\rho \gamma(x,\boldsymbol{R},\boldsymbol{\rho})$$
$$= \lim_{\rho\to 0}\lim_{N\to\infty}\sum_{k=1}^{N}\nabla_\rho \gamma_k(x,\boldsymbol{R},\boldsymbol{\rho}) = \lim_{N\to\infty}\sum_{k=1}^{N}\nabla_\rho \gamma_k(x,\boldsymbol{R},\boldsymbol{\rho})\big|_{\rho=0}. \quad (7)$$

Using the example of random displacements of the image of an optical source, we show how to regularise the singular phase. To do this, we represent the initial field, which we shall call a singular beam, in the form of a sum of elementary beams with an analytic phase. Then,

$$\nabla_\rho \gamma(x,\boldsymbol{R},\boldsymbol{\rho})\big|_{\rho=0} = \mathrm{i}\lim_{N\to\infty}\sum_{k=1}^{N} I_k(x,\boldsymbol{R})\nabla_R S_k(x,\boldsymbol{R}),$$
$$\gamma(x,\boldsymbol{R},0) = \lim_{N\to\infty}\sum_{k=1}^{N} I_k(x,\boldsymbol{R}), \quad (8)$$

where $I_k(x, \boldsymbol{R})$ and $S_k(x, \boldsymbol{R})$ are the intensity and phase of the elementary beam with the number k, respectively.

Let us consider in more detail the random component $\boldsymbol{\rho}_t'$ of the displacement vector of the centre of gravity of the image $\boldsymbol{\rho}_t$, corresponding to the random component of the phase $S_k'(x, \boldsymbol{R})$:

$$\boldsymbol{\rho}_t' = \frac{\lambda F_t}{2\pi p}\lim_{N\to\infty}\sum_{k=1}^{N}\int \mathrm{d}^2 R\, T(\boldsymbol{R}) I_k(x,\boldsymbol{R})\nabla_R S_k'(x,\boldsymbol{R}),$$
$$p = \int \mathrm{d}^2 R\, T(\boldsymbol{R})\gamma_k(x,\boldsymbol{R},0). \quad (9)$$

In expression (9), calculations are performed for an elementary beam carrying a random energy flux p.

Below, we use the ray approximation in (9), since it is known [2, 25] that it well describes the image jitter. In the ray approximation, the intensities $I_k(x,\boldsymbol{R})$ can be replaced by their mean values, i.e. $\langle I_k(x,\boldsymbol{R})\rangle$. Such a substitution is performed both in the numerator and in the denominator of expression (9). This means that the random flux p for the elementary beam in the denominator of (9) is also replaced by its mean value $\langle p\rangle$. It is known that in the ray approximation the random phase of the wave S' is represented [2] by the geometrical optics approximation with integration along the trajectory of the mean ray in the beam. Then, for the average intensity of any elementary beam (i.e., for all values of k) we have

$$\langle I_k(x,\boldsymbol{\rho})\rangle = \langle I_{\mathrm{eff}}(x,\boldsymbol{\rho} - \boldsymbol{\rho}_{k0}(1 - x/x^*)\rangle,$$
$$\langle I_{\mathrm{eff}}(x,\boldsymbol{\rho})\rangle = \frac{I_0 a_{\mathrm{eff}}^2(0)}{a_{\mathrm{eff}}^2(x)}\exp\left[-\frac{\rho^2}{a_{\mathrm{eff}}^2(x)}\right], \quad (10)$$

where $a_{\mathrm{eff}}(x)$ is the effective (average) radius of the elementary beam.

In the radiation plane ($x = 0$), the axis of such an elementary beam is at a distance $\boldsymbol{\rho}_{k0}$ from the X axis and intersects this axis at $x = x^*$. The point of intersection lies on the positive and negative semi-axes of X for $x^* > 0$ and $x^* < 0$, respectively. Below, all elementary beams are assumed to be identical for simplicity. They differ from each other only in the position of their axes, given by the vector $\boldsymbol{\rho}_{k0}$ in the initial plane. In the ray approximation, the random phase of the wave, S_k', is represented by a geometrical optics approximation with integration of the deviation of the random dielectric constant of the medium from unity along the path of the mean ray, $P'(x', x, \boldsymbol{\rho})$, i.e., the value $\varepsilon_1 = \varepsilon - 1$. Then, the random phase of the elementary beam with the number k has the form:

$$S_k'(x,\boldsymbol{\rho}) = \frac{\pi}{\lambda}\int_0^x \mathrm{d}x'\varepsilon_1(x',\, P_k(x',x,\boldsymbol{\rho})), \quad (11)$$

where

$$P_k(x',\, x,\boldsymbol{\rho}) = \boldsymbol{\rho}_{0k} f(x',\, x) + \boldsymbol{\rho} l_{\mathrm{eff}}(x',\, x);\; P_k(x,x,\boldsymbol{\rho}) = \boldsymbol{\rho};$$
$$f(x',\, x) = 1 - l_{\mathrm{eff}}(x',\, x) + (x/x^*)[l_{\mathrm{eff}}(x',\, x) - x'/x];$$
$$f(x,x) = 0;\; l_{\mathrm{eff}}(x',\, x) = a_{\mathrm{eff}}(x')/a_{\mathrm{eff}}(x).$$

The quantities $\langle I_k(x,\boldsymbol{\rho})\rangle$ and $S_k'(x,\boldsymbol{\rho})$ chosen in this way [by formulas (9) and (10)] allow us to consider as a superposition the sum of identical elementary beams whose axes intersect the X axis at point $x = x^*$ and are located at different distances $\boldsymbol{\rho}_{k0}$ from this axis in the initial plane $x = 0$.

Passing to the integrals, using the Gaussian profile for the receiving device's transmission coefficient of form $T(\boldsymbol{R}) = T_0\exp(-R^2/a_t^2)$, we obtain from (9) a regularised representation for $\boldsymbol{\rho}_t'$:

$$\boldsymbol{\rho}_t' = \frac{F_t}{2P}\int_0^x \mathrm{d}x' l_{\mathrm{eff}}(x',\, x)\int \mathrm{d}^2 R\nabla_\perp \varepsilon_1(x',\, \boldsymbol{R})\langle I(x',\, x,\boldsymbol{R})\rangle, \quad (12)$$

where

$$\langle I(x',\, x,\boldsymbol{R})\rangle = I_0\frac{a_R^2(x,x)}{a_R^2(x',\, x)}\exp(-R^2/a_R^2(x',\, x));$$
$$P = I_0\pi a_R^2(x,x) = I_0\pi a_1^2(x);\; a_R^2(x',x) = [a_t^2 a_\Sigma^2(x')$$
$$+ a_{\mathrm{eff}}^2(x)a^{*2}f^2(x',x)]/[a_t^2 + a_\Sigma^2(x)];\; a_\Sigma^2(x) = a_{\mathrm{eff}}^2(x)$$
$$+ a^{*2}(1 - x/x^*)^2;\; a_R^2(x,x) = a_t^2 a_\Sigma^2(x)/[a_t^2 + a_\Sigma^2(x)]$$
$$= a_1^2(x);\; a_1^{-2}(x) = a_t^{-2} + a_\Sigma^{-2}(x);$$

$T_0 = \mathrm{const}$; a_t is the radius of the receiving telescope; a^* is the radius of the incoherent source; and $a_\Sigma(x)$ is the effective radius of the composite beam, which is the sum of elementary beams with an analytic phase.

As a result, we obtain expression (12), in form coinciding with the representation of the vector $\boldsymbol{\rho}_t'$ for the case when the phase is analytic and the regularisation is not required, namely, with the form:

$$\boldsymbol{\rho}_t' = \frac{F_t}{k\langle P\rangle}\int \mathrm{d}^2\rho\, T(\boldsymbol{\rho})\langle I(x,\boldsymbol{R})\rangle\nabla_\rho S'(x,\boldsymbol{\rho})$$
$$= \frac{F_t}{kP_t}\int_0^x \mathrm{d}x' l(x',\, x)\int \mathrm{d}^2 R\nabla_\perp \varepsilon_1(x',\, \boldsymbol{R})\langle I_t(x',\, x,\, \boldsymbol{R})\rangle, \quad (13)$$

where

$$l(x',\, x) = a_{\text{eff}}(x')/a_{\text{eff}}(x);\ \langle I(x,\, x', \boldsymbol{R})\rangle = I_0 \frac{a_{\text{t}}^2(x,x)}{a_{\text{t}}^2(x',\, x)}$$

$$\times \exp\left(\frac{-R^2}{a_{\text{t}}^2(x',\, x)}\right);\quad P_{\text{t}} = I_0 \pi a_{\text{t}}^2(x,x) = I_0 \pi a_0^2(x);$$

$$a_{\text{t}}^2(x',\, x) = a_{\text{t}}^2 a_{\text{eff}}^2(x')/[a_{\text{t}}^2 + a_{\text{eff}}^2(x')] = a_0^2(x) l^2(x',\, x);$$

$$a_0^{-2}(x) = a_{\text{eff}}^{-2}(x) + a_{\text{t}}^{-2}.$$

Thus, a singular incoherent beam of radius a is easily approximated by the sum of elementary beams propagating from the initial plane $x = 0$, each of which has an initial radius equal to the coherence radius of the original incoherent singular beam [$a_{\text{eff}}(0) = \rho_k \to 0$]. In this case, we can assume in (12) that $a = a^*$ and the axes of all elementary pencils are parallel ($x^* \to \infty$). Strong diffraction divergence leads to the fact that the radius of the elementary beam at the end of the path is much larger than at the beginning, $a_{\text{eff}}(x) \gg a^*$. Therefore, in expressions (12) and (13) we can set

$$l^2(x',x) = x'/x,\quad a_{\Sigma}^2(x) = a_{\text{eff}}^2(x),$$

$$a_{\text{t}}^2(x',\, x) = (x'/x) a_{\text{t}}^2 + a_{\text{t}}^2(x) + (1 - x'/x)^2 a^2. \tag{14}$$

6. Image jitter of extended incoherent astronomical sources

Using representation (13) of the energy centre of gravity (vector ρ_{t}'), we can calculate the cross-correlation function $B(\boldsymbol{\rho}_{\text{t1}}', \boldsymbol{\rho}_{\text{t2}}') = \langle \boldsymbol{\rho}_{\text{t1}}'\, \boldsymbol{\rho}_{\text{t2}}' \rangle$ of two such vectors, $\boldsymbol{\rho}_{\text{t1}}$ and $\boldsymbol{\rho}_{\text{t2}}$. In the calculations we use the model of the turbulence spectrum, which takes into account the finiteness of the outer scale of turbulence [2, 9, 24]:

$$\Phi_n(\kappa, \xi) = A_0 C_n^2(\xi) \kappa^{-11/3} [1 - \exp(-\kappa^2/\kappa_0^2(\xi))], \tag{15}$$

where $C_n^2(\xi)$ is the structural parameter of the refractive index of the atmosphere; κ is the wave number; $\kappa_0(\xi) = 2\pi/L_0(\xi)$; $L_0(\xi)$ is the outer scale of atmospheric turbulence; and $A_0 = 0.033$.

In this case, a turbulent medium is given by a set of atmospheric profiles of the structural parameter of the refractive index $C_n^2(\xi)$ and the outer turbulence scale $L_0(\xi)$, which are the functions of the coordinates along the propagation path of the optical wave.

Let us elaborate the optical scenario: suppose that two identical receiving telescopes are used, separated by a distance $\boldsymbol{R}$ in the observation plane, provided with the same instruments that measure the centre of gravity of the random displacement of images due to the turbulence of the atmosphere. These telescopes are aimed at two identical incoherent radiation sources, spaced by a distance $\boldsymbol{\rho}$ in the original plane. Incoherent sources and receiving telescopes are separated from one another by a distance x. The entire space between the initial plane and the viewing plane is filled with a turbulent medium. Proceeding from such a scenario, the authors of Refs [24, 25] calculated the cross-correlation function $B(\boldsymbol{\rho}_{\text{t1}}', \boldsymbol{\rho}_{\text{t2}}')$ of random displacements $\boldsymbol{\rho}_{\text{t1}}'$ and $\boldsymbol{\rho}_{\text{t2}}'$ of two images of incoherent sources was calculated. Such a correlation function in the 'flat-Earth' approximation [2] is given in the form:

$$B(\boldsymbol{\rho}_{\text{t1}}', \boldsymbol{\rho}_{\text{t2}}') = B(x, \boldsymbol{\rho}, \boldsymbol{R}) = 2^{7/6} \pi^2 A_0 \Gamma(1/6) F_{\text{t}}^2$$

$$\times \int_0^x \mathrm{d}x' (1 - x'/x)^2 C_n^2(h_0 + x\cos\theta) \{[a_{\text{t}}^2 (1 - x'/x)^2$$

$$+ a^{*2} (x/x)^2]^{-1/6}\, {}_1F_1\left\{1/6, 1; -\frac{[\boldsymbol{R}(1 - x'/x) + \boldsymbol{\rho}(x'/x)]^2}{2[a_{\text{t}}^2 (1 - x'/x)^2 + a^{*2}(x/x)^2]}\right\} \tag{16}$$

$$- [a_{\text{t}}^2 (1 - x'/x)^2 + a^{*2}(x/x)^2 + 2\kappa_0^{-2}(h_0 + x'\cos\theta)]^{-1/6}$$

$$\times\, {}_1F_1\left\{1/6, 1; -\frac{[\boldsymbol{R}(1 - x'/x) + \boldsymbol{\rho}(x'/x)]^2}{2[a_{\text{t}}^2(1-x'/x)^2 + a^{*2}(x/x)^2 + 2\kappa_0^{-2}(h_0 + x'\cos\theta)]}\right\},$$

where ${}_1F_1$ is the Gauss hypergeometric function; h_0 is the height of the location of receiving telescopes above the underlying surface; θ is the zenith angle of the centre between two incoherent sources; and x is the distance between the plane of the sources and the plane of observation.

This optical measurement scenario and formula (16) are the most common; simpler situations are also possible. Thus, if the incoherent source is only one and it is observed by two receivers, then $\boldsymbol{\rho} = 0$ and in formula (16) only the distance $\boldsymbol{R}$ between two receivers varies. If there are two sources and they are observed simultaneously by only one receiving telescope, then $\boldsymbol{R} = 0$ and only the distance $\boldsymbol{\rho}$ between two sources varies. For a point source (a spherical wave) $a^* = 0$, and we obtain the well-known expression for the correlation function of the displacement of images of two point sources, each taken by its own telescope. Using expression (16), it is possible to perform calculations for various scenarios of optical observations.

7. Calculation for astronomical paths

Let us consider the case of practical use of incoherent astronomical sources and the operation of the system through the entire thickness of the atmosphere. This case is realised, for example, when using sunspots for measuring the image jitter in the focal plane of a solar telescope. The measurements are carried out using a Shack–Hartmann wavefront sensor. In this case, in expression (16) it is necessary to pass to the limit $x \to \infty$. We introduce two new parameters: $a_0 = a^*/x$ is the angular radius of the receiving telescope and $\boldsymbol{\beta}_0 = \boldsymbol{\rho}/x$ is the angular distance between two astronomical extended incoherent sources. We also assume that atmospheric turbulence is described by the Kolmogorov model, i.e., $L_0(\xi) \to \infty$, then

$$B(\boldsymbol{R}, \boldsymbol{\beta}_0, \alpha_0) = 2^{7/6} A_0 \pi^2 \Gamma(1/6) F_{\text{t}}^2 \int_0^x \mathrm{d}x' C_n^2(h_0 + x'\cos\theta)$$

$$\times (a_{\text{t}}^2 + a_0^2 x'^2)^{-1/6}\, {}_1F_1\left[1/6, 1; -\frac{(\boldsymbol{R} + \boldsymbol{\beta}_0 x')^2}{2(a_{\text{t}}^2 + \alpha_0^2 x'^2)}\right], \tag{17}$$

where $\sigma_{\text{t}}^2 = B(0, \boldsymbol{\beta}_0, \alpha_0)$ is the image jitter variance.

Next, we present numerical estimates of the mutual jitter of two images for one extended incoherent astronomical source on inclined paths. They can be two images of the same sunspot, measured by two spatially separated sensors. For the Shack–Hartmanm sensor, these can be different sub-aper-

tures of the same sensor. It is easy to show from (17) that for $\beta_0 = 0$

$$B(\boldsymbol{R},0,\alpha_0) = 2^{7/6}A_0\pi^2\Gamma(1/6)F_t^2\int_0^x \mathrm{d}x' C_n^2(h_0 + x'\cos\theta)$$

$$\times (a_t^2 + a_0^2 x'^2)^{-1/6}{}_1F_1\left[1/6, 1; -\frac{R^2}{2(a_t^2 + \alpha_0^2 x'^2)}\right]. \qquad (18)$$

Then all the characteristics (18) become functions of one generalised parameter $a_0 h_{\mathrm{eff}}\sec\theta/a_t$. In numerical calculations we use the well-known generalised model of the vertical profile $C_n^2(h)$ [2, 25]:

$$C_n^2(h) = C_n^2(h_0)(h/h_0)^{-2/3}\exp(-h/h_{\mathrm{eff}}),\ h \geqslant h_0, \qquad (19)$$

where h_{eff} is the effective thickness of the turbulent atmosphere (for the model used, $h_{\mathrm{eff}} \approx 3200$ m); and h is the current height above the underlying surface.

Figures 1 and 2 present the results of numerical calculations of the correlation function and variance. Figure 1 shows the dependence of the ratio σ_t^2 to the variance of the jitter of a spherical wave $\sigma_{t,sp}^2 = B(x,0,0)$ on the angular size of an extended incoherent source α_0. It is seen that for a typical turbulence model and a typical size of a measuring telescope, ~15 cm, deviations from the jitter of a spherical wave will not exceed 5%–10% for an extended source with a size of no more than 20 arcsec.

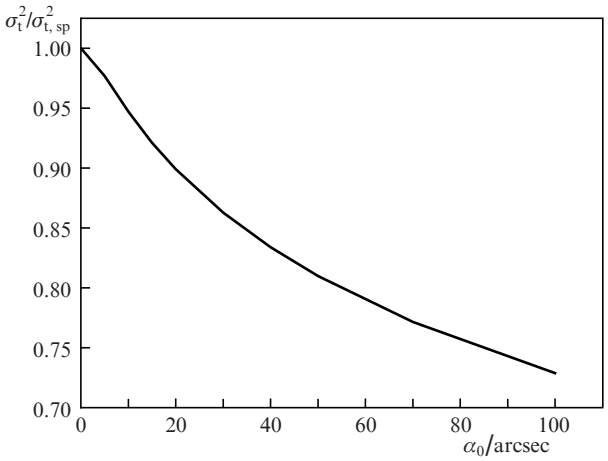

Figure 1. Dependence of the ratio $\sigma_t^2/\sigma_{t,sp}^2$ on the angular size of an astronomical extended source a_0. Here and in Figs 2 and 3, h_{eff} = 3200 m, h_0 = 6 m, $\theta = 45°$, a_t = 0.15 m.

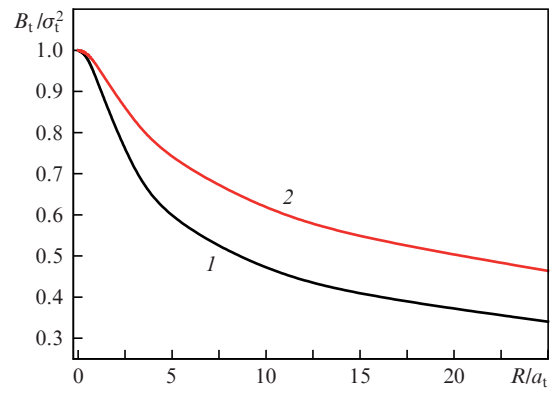

Figure 2. Dependences of the cross-correlation coefficient B_t/σ_t^2 on the normalised distance R/a_t between two receivers at a_0 = (*1*) 0 and (*2*) 100 arcsec.

Figure 2 shows the dependences of the cross-correlation coefficient of random displacements of images of an extended source with an angular size of 100 arcsec and a point source on the normalised distance between two receiving telescopes. In particular, it was found that even for $R/a_t \sim 10$, the correlation for an extended source differs significantly from that for the limiting case, i.e. a point object.

8. Operation of a Shack–Hartman wavefront sensor in the differential regime

Based on the results of the calculations performed, we can evaluate the efficiency and correctness of the operation of a differential turbulence meter using a signal from a Shack–Hartmann wavefront sensor, which represents a correlation Shack–Hartman sensor operating in the differential image motion monitor regime [26–28]. In this case, the differential circuit is formed by several pairs of segmented sub-apertures of the sensor. The use of such a sensor is equivalent to the following observation scheme: on an astronomical path there is an incoherent extended radiation source with a certain angular size. Such an object may be a solar pore, a sunspot or the edge of the solar disk. Let us distinguish in this sensor two identical receiving sub-apertures, which, for the sake of simplicity of further analysis, will be assumed to be Gaussian. Then, we can use the results of calculations [25] for vertical and inclined paths, on which turbulence is described by the Kolmogorov model. It is known that the differential measuring device actually estimates the average square of the difference of random displacements (the jitter effect) of two images characterised by two displacement vectors of the centre of gravity, $\boldsymbol{\rho}'_{t1}$ and $\boldsymbol{\rho}'_{t2}$, of two images, i.e., measures the magnitude of the structural function of the random angle of arrival $D(\boldsymbol{\rho}'_{t1}, \boldsymbol{\rho}'_{t2}) = \langle[\boldsymbol{\rho}'_{t1} - \boldsymbol{\rho}'_{t2}]^2\rangle$. In this case, the averaging $\langle[\boldsymbol{\rho}'_{t1} - \boldsymbol{\rho}'_{t2}]^2\rangle$ is performed over an ensemble of turbulent fluctuations.

For the variance of the difference $\langle[\boldsymbol{\rho}'_{t1} - \boldsymbol{\rho}'_{t2}]^2\rangle$, it is easy to obtain from (18) the expression

$$D(\boldsymbol{R},0,\alpha_0) = 2^{13/6}A_0\pi^2\Gamma(1/6)F_t^2\int_0^\infty \mathrm{d}x' C_n^2(h_0 + x'\cos\theta)$$

$$\times (a_t^2 + a_0^2 x'^2)^{-1/6}\left[1 - {}_1F_1\left(1/6, 1; -\frac{R^2}{2(a_t^2 + \alpha_0^2 x'^2)}\right)\right], \qquad (20)$$

which can be analysed from the point of view of the influence of the size of the incoherent extended source on the measurement data obtained with the help of this sensor. To simplify the analysis as much as possible, we consider the case of vertical paths, i.e., $\theta = 0$, and set also $h_0 = 0$; then,

$$D(\boldsymbol{R},0,\alpha_0) = 2^{13/6}A_0\pi^2\Gamma(1/6)F_t^2\int_0^\infty \mathrm{d}h C_n^2(h)$$

$$\times (a_t^2 + a_0^2 h^2)^{-1/6}\left[1 - {}_1F_1\left(1/6, 1; -\frac{R^2}{2(a_t^2 + \alpha_0^2 h^2)}\right)\right]. \qquad (21)$$

For the case of a point reference source, the parameter $\alpha_0 = 0$, and from (21) we obtain

$$D(\boldsymbol{R},0,0) = 2^{13/6}A_0\pi^2\Gamma(1/6)a_t^{-1/3}F_t^2\int_0^\infty dhC_n^2(h)$$

$$\times\left[1 - {}_1F_1\left(1/6,1;-\frac{R^2}{2a_t^2}\right)\right]. \quad (22)$$

This expression contains only two parameters, i.e., the size of the receiving apertures a_t and their mutual separation R. It is known that the degenerate Gauss hypergeometric function from (21), (22) has the following properties:

for small values of the argument ($R < a$)

$${}_1F_1\left(1/6,1;-\frac{R^2}{2a_t^2}\right) \approx 1 - \frac{R^2}{12a_t^2},$$

for large values of the argument ($R > a$)

$${}_1F_1\left(1/6,1;-\frac{R^2}{2a_t^2}\right) \approx \frac{1}{\Gamma(5/6)}\left(\frac{R^2}{2a_t^2}\right)^{-1/6}.$$

Then, for the most interesting case ($R > a$), we obtain from (22) the expression

$$D(\boldsymbol{R},0,0) = 2^{13/6}A_0\pi^2\Gamma(1/6)a_t^{-1/3}F_t^2$$

$$\times\left[1 - \frac{2^{1/6}}{\Gamma(5/6)}\left(\frac{R}{a_t}\right)^{-1/3}\right]\int_0^\infty dhC_n^2(h). \quad (23)$$

This formula is used by virtually all the developers of wavefront sensors to estimate the Fried radius. However, it is not difficult to see that for a telescope using extended objects on the Sun, the application of this formula can lead to an error. We will estimate it. To this end, formula (21) is calculated for the case of large separation of sub-apertures:

$$D(\boldsymbol{R},0,\alpha_0) = 2^{13/6}A_0\pi^2\Gamma(1/6)F_t^2$$

$$\times a_t^{-1/3}\int_0^\infty dhC_n^2(h)\left[\left(1+\frac{\alpha_0^2}{a_t^2}h^2\right)^{-1/6} - \frac{2^{1/6}}{\Gamma(5/6)}\left(\frac{R}{a_t}\right)^{-1/3}\right]. \quad (24)$$

To carry out a comparative analysis, it is necessary to introduce a model for the vertical evolution of the quantity $C_n^2(h)$, and also for the ratio between R and α_0. The simplest model for $C_n^2(h)$ is exponential, which has the form:

$$C_n^2(h) = C_n^2(0)\exp(-h/h_\xi), \quad (25)$$

where h_ξ is the effective atmospheric thickness of turbulence.

In analysing such a model, it is necessary to consider the relationships between the sizes of receivers a_t and the product $\alpha_0 h_\xi$. Note that the actual values of the parameters in question can be determined on the basis that the size a_t is usually chosen to be $\sim r_0$ (the Fried radius). Then, the size of the object in the image of the Sun must be limited by the condition:

$$\alpha_0 < r_0/h_\xi. \quad (26)$$

In the experiment, these two parameters entering into condition (26) are easily estimated: if the vertical profile of turbulence is known, they are calculated from the first moments of this profile:

$$r_0 \propto \left(\int_0^\infty dhC_n^2(h)\right)^{-3/5}, \quad h_\xi = \int_0^\infty dhhC_n^2(h)\Big/\int_0^\infty dhC_n^2(h). \quad (27)$$

However, as the analysis of various schemes for introducing AO systems into solar telescopes shows, not all equipment designers provide in practice the fulfilment of a simple condition (26). This, in turn, leads both to distortions in the work of the developed wavefront sensor and to errors in estimating the integral value of turbulence, and consequently, the Fried radius.

We shall calculate these possible errors by using formulas (23) and (24). Equating their values, we obtain the relation

$$\int_0^\infty d\hat{h}\hat{C}_n^2(h)\left[1 - \frac{2^{1/6}}{\Gamma(5/6)}\left(\frac{R}{a_t}\right)^{-1/3}\right]$$

$$= \int_0^\infty dhC_n^2(h)\left[\left(1+\frac{\alpha_0^2}{a_t^2}h^2\right)^{-1/6} - \frac{2^{1/6}}{\Gamma(5/6)}\left(\frac{R}{a_t}\right)^{-1/3}\right]. \quad (28)$$

Here, in the left-hand side, we have introduced the notation of the integral profile $\int_0^\infty d\hat{h}\hat{C}_n^2(h)$, measured with an error in view of the use of the assumption that the reference object is point-like, and in the right-hand side a correct estimate of the integral turbulence profile $\int_0^\infty dhC_n^2(h)$ is presented, which is obtained on the assumption that the object is extended. Then, from (28) we approximately obtain that this assumption leads to an underestimation of the ratio

$$\int_0^\infty d\hat{h}\hat{C}_n^2(h)\Big/\int_0^\infty dhC_n^2(h) = \left(1+\frac{\alpha_0^2}{a_t^2}h_\xi^2\right)^{-1/6} \quad (29)$$

by approximately $1 - {}^1/_6(\alpha_0^2/a_t^2)h_\xi^2$ times. For example, an estimate at a Fried radius of $r_0 = 5$ cm (for a wavelength of 0.55 μm) and an atmospheric turbulence thickness of h_ξ = 1000–1500 m yields that with an angular size of the reference object on the Sun, 3 and 5 arcsec, an understatement lies in the range from 5% to 30%. And this, accordingly, will overstate the estimate of the Fried radius. Formula (24) shows that a correct estimate of the integral profile of turbulence and, consequently, of the Fried radius can be obtained only in

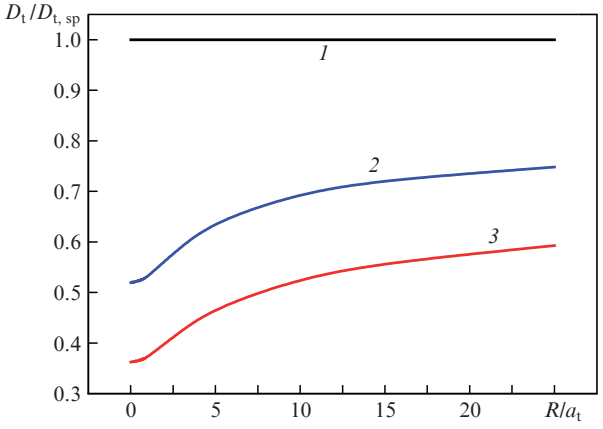

Figure 3. Dependences of the ratio of the structural displacement function of the image of one astronomical extended source to the structural displacement function of the image of the spherical wave on the normalised distance R/a_t between two receivers at a_0 = (*1*) 0, (*2*) 40 and (*3*) 100 arcsec.

the presence of information about the behaviour of the integral profile or moments (27).

Similar calculations were also performed numerically, using a more realistic model of atmospheric turbulence. Figure 3 shows the calculated dependences of the ratio of the structural function of a random displacement for the operation of a differential measuring device for objects of different sizes on the normalised distance between two receivers.

The results of these calculations provide complete information about the choice of the necessary separation of the two sub-apertures to ensure correct measurements of the integral profile of turbulence on a vertical path.

9. Experiment for vertical (astronomical) paths

To verify the theory's conclusions, we performed optical meteorological measurements at the Sayan Solar Observatory (Institute of Solar-Terrestrial Physics of the Siberian Branch of the Russian Academy of Sciences) using an automated horizontal solar telescope [26]. The design of the telescope includes a siderostat, i.e., a system of two flat mirrors 800 mm in diameter, which provides continuous tracking of the Sun. The siderostat reflects sunlight to the main spherical mirror 800 mm in diameter with a focal length of 18 m. The mirror constructs the image of the Sun on the photodetector. The variance of the image jitter σ_t^2 of the edge of the solar disk was measured as a function of the radius of the receiving mirror a_t. As a jitter measuring device, we used a Brandt photoelectric sensor, which was successfully tested for several decades and used previously in similar studies in Russia and abroad.

Simultaneously with optical measurements, the state of the atmosphere was controlled by a Meteo-3M mobile ultrasonic meteorological system. The main averaged parameters of the experiments are as follows: the zenith angle of the observed object, $\theta \approx 60°$; the structural characteristic of fluctuations of the refractive index at a height of 4.5 m from the underlying surface, $C_n^2 = 1.7\times10^{-15}$ cm$^{-2/3}$; the average surface wind speed, 6 m s^{-1}; and the angular size α_0 of the astronomical incoherent source (the edge of the solar disk) corresponding to the angular resolution of the receiver used varied from 0.1 to 1.5 arcsec.

The results of astronomical and parallel meteorological measurements have shown (Fig. 4) that when coherent turbulence is recorded in the atmosphere (the temperature fluctuation spectrum, $W_T \sim f^{-8/3}$) [26], our data coincides with the coherent theory [$\sigma_\alpha \approx$ const, open symbols and line (*3*) in Fig. 4]. In the case of incoherent Kolmogorov turbulence ($W_T \sim f^{-5/3}$), our results for a point source ($\alpha_0 = 0.1$ arcsec) coincide with the conventional Kolmogorov theory [filled symbols and line (*1*) in Fig. 4].

For Kolmogorov turbulence, the theoretical curve in Fig. 4 is plotted taking into account the regularisation of the image jitter of an incoherent extended source. This corresponds to taking into account the deviation of a real astronomical incoherent object (the edge of the solar disk) from the point one. As can be seen from Fig. 4, a satisfactory agreement of the theory with the experiment is observed. In accordance with theoretical data, the jitter of the image of the edge of the solar disk ($\alpha_0 \neq 0$) with decreasing diameter of the receiver $2a_t$ should approach a constant value; the standard deviation of the image jitter of the edge of the solar disk for Kolmogorov-type turbulence with decreasing receiver diameter $2a_t$ also tends to a constant value.

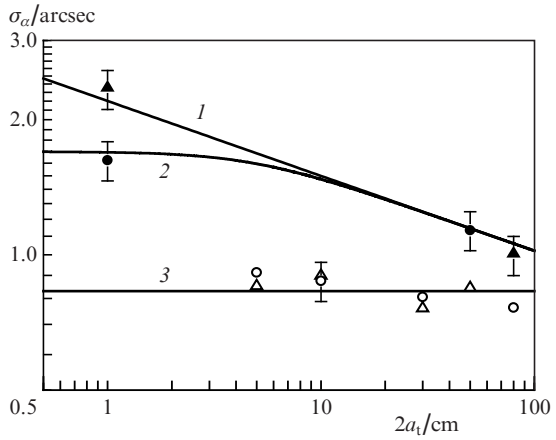

Figure 4. Dependences of the standard deviation σ_α of the angular jitter of the astronomical image of the edge of the solar disk on the diameter of the input aperture of the telescope $2a_t$ in the case of (○, △) coherent turbulence and (●, ▲) incoherent Kolmogorov turbulence for (▲, △; $\alpha_0 = 0.1$ arcsec) a point source and (●, ○; $\alpha_0 = 1.1$ arcsec) an extended incoherent source; (*1*) Kolmogorov turbulence and a point source, (*2*) the same for an extended source, (*3*) calculation for coherent turbulence conditions.

The data obtained with a Brandt sensor can be used to simultaneously determine the Fried radius r_0 and the effective outer scale of atmospheric turbulence. In paper [27], it is proposed to perform measurements of the variance of the jitter of the star image in the focal plane of the telescope simultaneously with several (at least two) values a_t of the receiving aperture of the telescope. In this case, an expression is used for the variance of the image jitter of the radiation source in the focal plane of the telescope, calculated for the model of atmospheric turbulence (15), which takes into account the finiteness of the magnitude of the outer scale of turbulence

$$\langle(\rho_t^{pl})^2\rangle \approx 3.23F_t^2 a_t^{-1/3} r_0^{-5/3} k^{-2}[1 - 2^{-1/6}(\kappa_0^* a_t)^{1/3}]. \quad (30)$$

The effective (integral) outer scale of turbulence $(\kappa_0^*)^{-1}$ in [27] was introduced on the basis of the formula:

$$(\kappa_0^*)^{-1} = \left[\int_0^\infty d\xi C_n^2(\xi)\kappa_0^{1/3} \Big/ \int_0^\infty d\xi C_n^2(\xi)\right]^{-3}. \quad (31)$$

10. Assessment of the requirements to the size of the reference source

Let us consider the requirements to a multichannel correlation Shack–Hartmann wavefront sensor of the. In analysing the situation, we will start from the formula that determines the dependence of the variance of the image jitter on the size of the sub-aperture and the size of the incoherent source itself. This leads to the fact that the variance of the random (linear) displacement of the image of such an incoherent source object σ_t^2, measured with a sensor having a receiving aperture of the effective radius a_t, on an inhomogeneous path (for example, propagating into the zenith) can be calculated from formulas (17) and (18).

It makes sense to consider two cases: a homogeneous path and a vertical path to an object located outside the atmosphere (in the case of an artificial Earth satellite). Using our

results, the expression for the variance of the image jitter (18) on the vertical path can be rewritten in the form:

$$\sigma_t^2 = \text{const}\, F_t^2 \int_0^\infty d\xi C_n^2(\xi)[a_t^2 + \xi^2\alpha_0^2]^{-1/6}. \quad (32)$$

Because the atmospheric turbulence is limited in length by the effective thickness [8, 15] of the atmospheric turbulence h_ξ, we obtain the condition, in which the receiver size a_t can be considered 'large' and the tracking object 'small':

$$a_t > \alpha_0 h_\xi. \quad (33)$$

It should be noted that since the measuring device of the image fragment displacement on the sub-aperture can react to the edge shift of the image, the angular 'image size' can be taken to be the minimum angular size that the optical system is capable of resolving. Let us consider a hypothetical case when the tracking object has many contrasting fragments, allowing one to measure the jitter of its image. Then, when the system operates under turbulent conditions, the minimum angular size of the object beyond which the tracking can be performed is the limiting angular resolution for the optical system in a turbulent medium, namely, λ/r_0^{se}, where r_0^{se} is the radius of coherence of the turbulent atmosphere under 'a short exposure'; and λ is the wavelength of the radiation. In this case, condition (33), to which the minimum required size of the sensor sub-aperture must satisfy, transforms to the condition:

$$a_t > \lambda h_\xi / r_0^{se}. \quad (34)$$

It is known that always $r_0^{se} > r_0$ [24, 25]. From the analysis of the last expression, it is easy to conclude that if for a vertical atmospheric path we use a minimally resolved object under a short exposure as the size of an effective tracking object, then such an object can be considered almost point-like. Indeed, such an object can be effectively used to measure and correct the phase.

For example, we will use the following values: let the thickness (height) of the turbulent atmosphere be $h_\xi = 2$ km and the radius of coherence under 'a short exposure', r_0^{se}, be set for the visible wavelength range of 10 cm. We then obtain from (34) that the necessary minimum size of the sensor sub-aperture reduced to the input aperture should be greater than 1 cm.

Let us analyse this problem for homogeneous paths [when $C_n^2(\xi) = C_n^2$)] in the case of Kolmogorov-type turbulence. In this case, expression (32) transforms into

$$\sigma_t^2 \approx 4F_t^2 C_n^2 X \int_0^1 d\xi (1-\xi)^2[(1-\xi)^2 a_t^2 + \xi^2 b^2]^{-1/6}. \quad (35)$$

Thus, for small linear sizes of the incoherent source object ($b < a_t$), such that we can use in (35) the expansion in a series with respect to the small parameter b/a_t, we obtain

$$\sigma_t^2 \approx 4F_t^2 C_n^2 X a_t^{-1/3} \left\{ \int_0^1 d\xi (1-\xi)^{5/3} - \frac{b^2}{6a_t^2} \int_0^1 d\xi (1-\xi)^{-1/3} \xi^2 \right\}. \quad (36)$$

Calculating the integrals in (36), we arrive at the expression

$$\sigma_t^2 \approx \frac{3}{2} F_t^2 C_n^2 X a_t^{-1/3} \left(1 - 0.4 \frac{b^2}{a_t^2}\right). \quad (37)$$

Because the first term in (37) is an expression for the variance of the displacement of the point-source image at the aperture, it is seen that with an increase in the linear size of the reference source b, there is a slight decrease in the useful signal in comparison with the case of a point source. If in expression (35) we put, for example, $b = d$, we obtain

$$\sigma_t^2 = 4F_t^2 C_n^2 X a_t^{-1/3} \int_0^1 d\xi (1-\xi)^2[(1-\xi)^2 + \xi^2]^{-1/6}. \quad (38)$$

An approximate calculation of integral (38) gives

$$\int_0^1 d\xi (1-\xi)^2[(1-\xi)^2 + \xi^2]^{-1/6} \approx 1/3.$$

Thus, the signal level indeed decreases, since $1/3 < 3/8$; however, this decrease is insignificant. Therefore, it turns out that on a horizontal path, even in conditions when the size of the receiver becomes comparable with the linear size of the source ($b = a_t$), the signal level of the image jitter decreases only by 6%. We can make an interesting conclusion: on horizontal paths, the dependence of the jitter signal weakly depends on the size of the incoherent source.

Let us emphasise once again that in these estimates the parameter a_t is the size of the wavefront sensor sub-aperture, reduced to the input of the optical system. It is precisely when condition (34) is satisfied for each of the channels of the wavefront sensor that a measurement, analogous to the measurement by the sensor as a whole in the case of a spherical wave, is performed [25–27]. It should be noted that in some works on the use of wavefront sensors for solar telescopes, the angular size of a separate sub-aperture is in the range of 8–20 arcsec [28, 29]. If we assume that the height of the atmosphere, h_ξ, is from 1 to 2 km, then using formula (21) instead of formula (22), taking into account the finite size of the tracking region, can be sufficiently justified only for sufficiently strong turbulence. For example, r_0 should be greater than 7–10 cm, so that condition (31) can be met. As our analysis [26, 27] shows, this condition does not always take place in reality; therefore, instead of formula (21), use should be made of formula (22) in processing the signal from the wavefront sensor, in which the finiteness of the tracking region is taken into account. Correct allowance for this factor requires a preliminary study of the structure of turbulence in the region [26, 27]. The dependence of the image jitter on the wavelength of reference radiation can be also taken into account, for example, as in [30].

11. Conclusions

We have presented a scheme of the operation of an adaptive optical system that does not require the creation or formation of a special reference source. The adaptive system uses the tracking of an image of a self-luminous object or an object illuminated by extraneous sources. Note that for the effective operation of the correlation sensor during tracking, we should use the smallest but the most contrasting element of the image. In the atmosphere on long paths, a strong aerosol blur of the reference source image is possible, and only a sufficiently extended object, i.e., an object with low spatial frequencies, will be clearly visible against the background of

other objects. This is due to the fact that the frequency-contrast characteristic of the aerosol atmosphere has a maximum in the low-frequency region and decreases at high spatial frequencies [31]. The deterioration in the visibility of the object due to the presence of aerosol frequencies in the atmosphere reduces the potential of this measuring device.

In general, we have shown the possibility of employing a Shack–Hartmann correlation sensor in adaptive systems using the image of an object (or its fragment) as a reference source.

Acknowledgements. The work was partially supported by the Russian Science Foundation (Grant No. 15-19-20013).

References

1. Fried D.L. *J. Opt. Soc. Am.*, **56** (10), 1380 (1966).
2. Gurvich A.S., Kon A.I., Mironov V.L., Khmelevtsov S.S. *Lazernoe izluchenie v turbulentnoi atmosphere* (Laser Radiation In a Turbulent Atmosphere) (Moscow: Nauka, 1976).
3. Linnik V.P. *Opt. Spektrosk.*, **25** (4), 401 (1957).
4. Hardy J.W. *Proc. IEEE*, **66**, 651 (1978).
5. Lukin V.P. *Sov. J. Quantum Electron.*, **10** (6), 727 (1980) [*Kvantovaya Elektron.*, **7** (6), 1270 (1980)].
6. Lukin V.P. *Sov. J. Quantum Electron.*, **11** (10), 1311 (1981) [*Kvantovaya Elektron.*, **8** (10), 2145 (1981)].
7. Lukin V.P., Charnotskii M.I. *Sov. J. Quantum Electron.*, **12** (5), 602 (1982) [*Kvantovaya Elektron.*, **9** (5), 952 (1982)].
8. Lukin V.P., Matyukhin V.F. *Sov. J. Quantum Electron.*, **13** (12), 1604 (1983) [*Kvantovaya Elektron.*, **10** (12), 2465 (1983)].
9. Lukin V.P. *Atmosfernaya adaptivnaya optika* (Atmospheric Adaptive Optics) (Novosibirsk: Nauka, 1986).
10. Lukin V.P., Fortes B.V. *Adaptivnoe formirovanie puchkov i izobrazhenii v atmosphere* (Adaptive Formation of Beams and Images In the Atmosphere) (Novosibirsk: Institute of Atmospheric Optics, Sib. Branch of RAS, 1999).
11. Lukin V.P. *In the collection of works 'How it was...'* (Moscow: LAS, 2016) Vol. 5, p. 181.
12. Greenwood D.P. *Lincoln Lab. J.*, **5** (1), 3 (1992).
13. *Scintillation. International Meeting for Wave Propagation in Random Media* (Seattle, WA, USA, 1992).
14. Foy R., Labeyrie A. *Astronomy & Astrophysics*, **152**, L29 (1985).
15. Lukin V.P. *Proc. SPIE*, **5743**, 50 (2004).
16. Lukin V.P. *Opt. Atmos. Okeana*, **19** (12), 1021 (2006).
17. Lukin I.P. *Opt. Atmos. Okeana*, **28** (4), 298 (2015).
18. Lukin V.P. *J. Opt.*, **15** (4), 044009 (2013).
19. Khizhnyak A.I., Markov V.B. *Proc. SPIE*, **8238**, 82380K-1 (2012).
20. Lukina N.P. *Proc. SPIE*, **4338**, 4 (2001).
21. Lukin V.P. *Opt. Atmos. Okeana*, **26** (2), 175 (2013).
22. Michau V., Rousset G., Fontanella J.C. *Proc. of Workshop on Real-Time and Post-Facto Solar Image Correction* (NSO, Sacramento Peak, USA, 1992) p. 91.
23. Lukin V.P., Charnotskii M.I. *Opt. Spektrosk.*, **66** (5), 1131 (1989).
24. Mironov V.L., Nosov V.V., Chen B.N. *Izv. Vyssh. Uchebn. Zaved., Ser. Radiofiz.*, **23** (4), 461 (1980).
25. Nosov V.V. *Doct. Diss.* (Tomsk, 2010).
26. Nosov V.V., Grigor'ev V.M., Kovadlo P.G., Lukin V.P., Nosov E.V., Torgaev A.V. *Vestn. MSTU 'Stankin'*, No. 1, 103 (2013).
27. Lukin V.P., Nosov V.V., Torgaev A.V. *Appl. Opt.*, **53** (10), B196 (2014).
28. Noriaki Miura, Akira Oh-ishi, Susumu Kuwamura, Naoshi Baba, Yoichiro Hanaoka, Satoru Ueno, Yoshikazu Nakatani, Kiyoshi Ichimoto. *Proc. SPIE*, **9909**, 99092N (2016).
29. Dirk Schmidt, Thomas Rimmele, Jose Marino, Friedrich Wöger. *Proc. SPIE*, **9909**, 99090X (2016).
30. Lukin V.P. *Appl. Opt.*, **48** (1), A93 (2009).
31. Zuev V.E., Belov V.V., Veretennikov V.V. *Theory of Systems in the Optics of Dispersion Media* (Tomsk: Institute of Atmospheric Optics, Sib. Branch of RAS, 1997).